

# Control of optical-feedback-induced laser intensity noise in optical data recording

**George R. Gray**  
**Andrew T. Ryan**  
**Govind P. Agrawal**  
Institute of Optics  
University of Rochester  
Rochester, New York 14627

**Edward C. Gage**  
Eastman Kodak Company  
Rochester, New York 14652

**Abstract.** The usefulness of semiconductor lasers can be greatly limited when the laser is subjected to uncontrolled optical feedback (OFB). In particular, the laser intensity noise can be severely degraded when OFB is greater than 0.1%. Although the technique of high-frequency injection (HFI) can solve this problem, the proper modulation frequency and depth must be chosen empirically. We investigate this problem through computer simulations of the multimode stochastic rate equations, modified to include OFB and HFI. By providing the program with measurable laser and system parameters, the simulations predict the HFI modulation frequency and depth that optimize the laser behavior. The results of the simulations are compared with experiment, and good agreement is obtained.

*Subject terms: optical data recording; optical feedback; semiconductor lasers.*  
*Optical Engineering 32(4), 739-745 (April 1993).*

## 1 Introduction

Semiconductor lasers are commonly used for storage and retrieval of information in optical data recording systems. A measure of the importance of this emerging optoelectronic technology is provided by the compact-disc players that have already penetrated the consumer electronics market. The same technique is now being extended to the mass storage devices capable of storing gigabytes of information on a single optical disk. Although optical disk-based mass storage devices are already available commercially, several technological problems must be solved to further improve their performance. One such problem is related to the control of relative intensity noise (RIN) of semiconductor lasers used inside the optical head for reading and writing the data to the optical disk.

The RIN of a well-designed semiconductor laser isolated from external reflections is typically low<sup>1,2</sup> enough ( $< 120$  dB/Hz) so that it can be used successfully in optical data recording systems. Unfortunately, it is often the case that a small fraction of the laser output is invariably fed back into the semiconductor laser because of the reflection occurring at the disk surface. Figure 1 shows the schematic design of an optical head used for reading and writing the data to the optical disk. To minimize the optical feedback

(OFB) into the laser diode, a combination of the polarization beamsplitter and a quarter-wave plate is used as an optical isolator. Indeed, the feedback should be absent if the isolator worked perfectly for all laser wavelengths and if the reflection from the optical disk were polarization independent. Unfortunately, the optical substrate is often birefringent; hence, a fraction of the laser output is fed back into the semiconductor laser. Experiments show that the RIN is increased by 20 dB or more as a result of this feedback. The increase in RIN degrades<sup>3</sup> the SNR and severely impacts the performance of optical recording systems.

Attempts have been made to suppress the feedback-induced RIN enhancement in the optical head. In a simple scheme known as the high-frequency injection technique,<sup>4-9</sup> the laser current is modulated sinusoidally at frequencies much higher than the data rate. The experimental results show that the RIN increase does not occur if the modulation frequency is suitably optimized and if the modulation amplitude is large enough to ensure that the laser is below threshold during a part of the modulation cycle.

Unfortunately, the optimum values of the modulation frequency and amplitude need to be determined empirically because a theoretical understanding has been lacking. In this paper, we present a rate equation model that is capable of explaining why the RIN is increased, and why this increase can be avoided through high-frequency injection. Computer simulations are used to find the optimum parameters for controlling the laser intensity noise. The results are compared with the experimental data.

Paper ET-015 received Nov. 5, 1992; revised manuscript received Nov. 10, 1992; accepted for publication Dec. 4, 1992.  
© 1993 Society of Photo-Optical Instrumentation Engineers. 0091-3286/93/\$2.00.

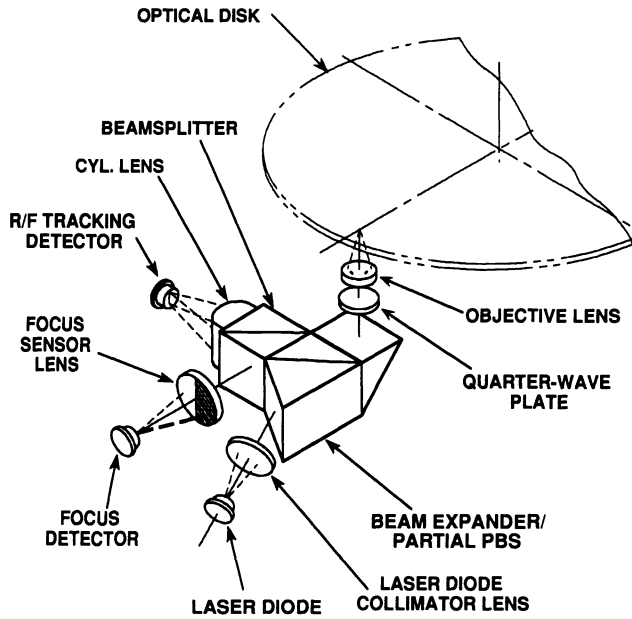


Fig. 1 Schematic of typical optical recording head.

## 2 The Rate Equation Model

The noise characteristics such as the RIN, the frequency noise, and the spectral linewidth, can be studied by using a rate equation model that includes the effect of spontaneous-emission noise and shot noise through a random term added to each rate equation.<sup>1,2</sup> The effects of optical feedback and high-frequency injection can also be included in this model in a straightforward manner. In the general case of a multimode semiconductor laser, these rate equations can be written as

$$\frac{dE_m}{dt} = -\frac{1}{2}(1 - i\alpha)(G_m - \gamma_m)E_m + \zeta_m^{int} + F_m(t) + \kappa_m E_m(t - \tau) \exp(i\omega_m \tau) \quad (1)$$

$$\frac{dN}{dt} = \frac{I}{q} - \frac{N}{\tau_e} - \sum_{j=1}^M G_j |E_j|^2 + F_N(t) \quad (2)$$

where

$$G_m(N) = A(N - N_0) - \delta G_m \quad (3)$$

$$\zeta_m^{int} = -\frac{1}{2} \left( \beta_m P_m + \sum_k \theta_{mk} P_k \right) E_m + \sum_k \kappa_{mk} E_{2k-m} E_k^2 \quad (4)$$

In Eq. (1),  $E_m(t)$  is the complex amplitude of the  $m$ 'th mode oscillating at the frequency  $\omega_m$ ,  $G_m$  is the mode gain,  $\gamma_m$  is the mode-dependent cavity loss,  $\zeta_m^{int}$  accounts for interaction among laser modes through various processes such as self-saturation, cross saturation, and four-wave mixing, and  $F_m(t)$  is the random noise generated through spontaneous emission. The complex electric field is written in terms of amplitude and phase as  $E_m(t) = [P_m(t)]^{1/2} \exp[-i\phi(t)]$ , where  $P_m$  and  $\phi$  are the photon number and phase, respectively, of the  $m$ 'th mode. In Eq. (2),  $N$  is the

electron number inside the active region of the semiconductor laser,  $I$  is the injection current,  $q$  is the electron's charge,  $\tau_e$  is the carrier lifetime, and  $F_N(t)$  is the random noise from carrier generation and recombination (shot noise). In Eqs. (3) and (4),  $A$  is the gain parameter related to the rate at which the peak gain increases with increasing  $N$ ,  $N_0$  is the transparency value of  $N$ ,  $\delta G_m$  is the gain margin related to the offset of the mode from the gain peak,  $\beta_m$  is the self-saturation parameter,  $\theta_{mk}$  is the cross-saturation parameter, and  $\kappa_{mk}$  is the four-wave-mixing parameter. The numerical values of  $\beta_m$ ,  $\theta_{mk}$ , and  $\kappa_{mk}$  depend on the mechanism responsible for the mode interaction. Their expressions are well known for the case in which the mode interaction occurs because of intraband nonlinearities related to spectral hole burning.<sup>10</sup> Other mechanisms such as carrier heating and two-photon absorption can be easily included. Although four-wave-mixing coupling is included in Eq. (1), we neglect such coupling for this paper, because its effect is expected to be small.

The effect of OFB is included through the last term in Eq. (1). The feedback parameter  $\kappa_m$  is given by<sup>11</sup>

$$\kappa_m = \frac{(1 - R_m)}{\tau_{Lm}} \left( \frac{\eta_{cm} \text{OFB}}{R_m} \right)^{1/2} \quad (5)$$

where OFB is the fraction of output power that is reflected back toward the laser facet facing the polarization beamsplitter (see Fig. 1). Also,  $R_m$  is the reflectivity of the facet facing the external cavity,  $\tau_{Lm}$  is the round-trip time of  $m$ 'th mode in the laser cavity, and  $\eta_{cm}$  is the coupling efficiency of the returned light into the active region. Both  $\tau_{Lm}$  and  $\eta_{cm}$  are nearly the same for all modes, and can be assumed to be mode independent to a good approximation. In contrast, the phase shift  $\omega_m \tau$  in the external cavity, with  $\tau = 2L_{ext}/c$  being the round-trip time from the laser facet to the optical disk, is not the same for all modes because of their different frequencies  $\omega_m$ . It is useful to write  $\omega_m$  as

$$\omega_m = \omega_c + (m - m_0)\Delta\omega_L \quad (6)$$

where  $\omega_c$  is the angular frequency of the central mode located at  $m = m_0$  and  $\Delta\omega_L/2\pi$  is the longitudinal-mode spacing ( $\sim 100$  GHz). For the coupling constant, we will use a value of  $\eta_c = 2\%$ , as estimated by comparison to the experimental measurements.

The rate Eqs. (1) and (2) can be used to obtain the RIN of the diode laser in the presence of optical feedback by integrating them numerically and calculating the spectrum of intensity fluctuations. If  $P_m(t)$  is the  $m$ 'th mode photon number, and  $\bar{P}_m$  is its average value, the RIN spectrum is defined as the Fourier transform of the autocorrelation function according to the relation

$$S_m(\omega) = \frac{1}{\bar{P}_m^2} \int_{-\infty}^{\infty} \langle \delta P_m(t) \delta P_m(t+t') \rangle \exp(-i\omega t') dt' \quad (7)$$

where  $\delta P_m(t) = P_m(t) - \bar{P}_m$  is the fluctuation at time  $t$ . Equation (7) provides RIN for a specific laser mode. In the optical recording systems the individual modes are not distinguished. Rather, the system performance is governed by the total photon number,

$$P_T(t) = \sum_{m=1}^M P_m(t) .$$

The RIN for the total photon number is obtained by replacing  $P_m$  by  $P_T$  in Eq. (7), and is given by

$$S_T(\omega) = \frac{1}{\bar{P}_T^2} \int_{-\infty}^{\infty} \langle \delta P_T(t) \delta P_T(t+t') \rangle \exp(-i\omega t') dt , \quad (8)$$

where  $\bar{P}_T$  is the total average photon number. The photon number can be converted to the optical power by using the well-known relation given, for example, in Refs. 1 and 2.

In the next section we present the results for the total RIN,  $S_T(\omega)$ , obtained by integrating the rate Eqs. (1) and (2) numerically. The parameter values used correspond to a typical index-guided GaAlAs semiconductor laser likely to be used in optical recording systems. These values are listed in Table 1, and result in a threshold current of 61 mA and a slope efficiency of about 0.5 mW/mA. Most of the simulations are presented for a constant output power of 1.6 mW, a typical value used for reading data from an optical disk. We include five longitudinal modes in our numerical simulations, which are performed using a fourth-order Runge-Kutta algorithm. The RIN spectra are calculated from time series of lengths 30 to 500 ns, depending on the resolution desired, after the transients have died out. The spectra are averaged over several trajectories to improve numerical accuracy. The effect of high-frequency injection is included by replacing the current  $I$  in Eq. (2) by

$$I(t) = I_b + I_m \sin(2\pi f_m t) , \quad (9)$$

where  $I_b$  is the bias current,  $I_m$  is the modulation current, and  $f_m$  is the frequency of sinusoidal modulation.

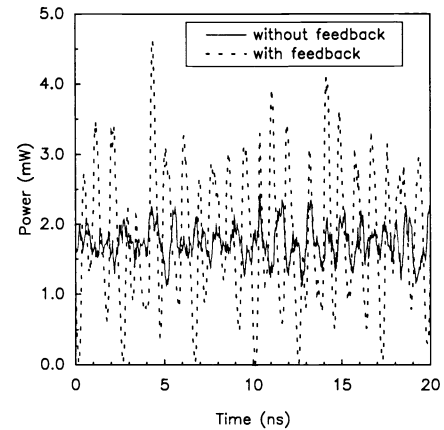
### 3 Effect of Optical Feedback on Laser Dynamics

Optical feedback (OFB) affects the noise and dynamics of the laser in different ways, depending on the length of the external cavity and the strength of the feedback. It is common to divide these different effects into five regimes of feedback.<sup>12</sup> For the levels of OFB common in optical recording systems, we are interested primarily in regimes II through IV. Briefly, regime II is characterized by mode hopping between external cavity modes, regime III by the possibility of frequency locking to one mode of the external cavity, and regime IV by a drastic reduction of the laser coherence length ("coherence collapse") caused by the severe broadening of the laser line. The OFB in write-once optical data recording systems is typically in the range 0.1 to 2%, falling into the regimes II through IV.

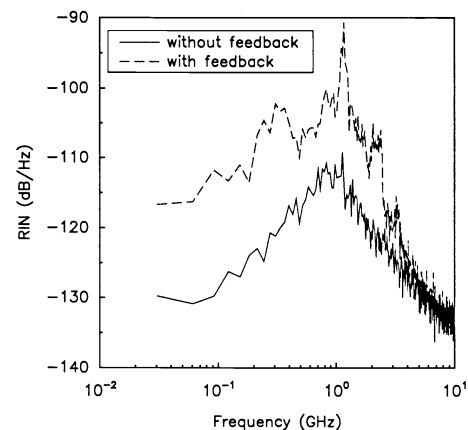
Before considering the multimode case, it is useful to consider the case of a semiconductor laser oscillating in a single longitudinal mode. The laser power as a function of time for  $L_{ext} = 10$  cm and 1% OFB is shown in Fig. 2(a); the associated RIN spectra are shown in Fig. 2(b). The laser power for 1% OFB fluctuates far more than the case of no feedback, which is also shown for comparison. In addition, the output appears somewhat periodic, although the peak heights are randomly distributed. The associated RIN spectra for the two cases with and without feedback are shown

**Table 1** Typical parameter values of a 780 nm GaAlAs laser used in optical recording.

PARAMETER	SYMBOL	VALUE
Longitudinal mode spacing	$\Delta\omega_L/2\pi$	107 GHz
Solitary laser roundtrip time	$\tau_L$	9.3 ps
Linewidth-enhancement factor	$\alpha$	4
Laser facet reflectivities	$R_1, R_2$	0.9, 0.12
Mode loss rate (using internal loss of 65 cm <sup>-1</sup> )	$\gamma_m$	$5.9 \times 10^{11} \text{ s}^{-1}$
External cavity length	$L_{ext}$	10 cm
External cavity roundtrip time	$\tau$	0.67 ns
Carrier recombination time	$\tau_c$	2 ns
Gain coefficient	$A$	$1193 \text{ s}^{-1}$
Transparency carrier number	$N_0$	$1.64 \times 10^8$
Self-saturation coefficient	$\beta_m$	$4.7 \times 10^3 \text{ s}^{-1}$
Cross-saturation coefficient	$\theta_{mk}$	$4.4 \times 10^3 \text{ s}^{-1}$
Bias current	$I_B$	~ 65 mA
Average output power	~	1.6 mW
Coupling efficiency	$\eta_c$	2%



(a)



(b)

**Fig. 2** Simulated temporal power variations (a) and the corresponding RIN spectra (b) for a single-mode laser without feedback (solid line) and with 1% OFB (dashed line).

in Fig. 2(b). The RIN without feedback has a low value (approximately  $-130$  dB/Hz) for frequencies below 100 MHz, and shows a broad peak near 800 MHz, which corresponds to the relaxation-oscillation frequency. When OFB of 1% is added, the peak associated with the relaxation oscillations shifts to a lower frequency and becomes somewhat undamped. In addition, there is a sharp higher frequency peak above 1 GHz, but slightly lower than the external cavity mode spacing of 1.5 GHz. The feature of the RIN with feedback that is most important for optical recording is the nearly 15 dB enhancement of the low-frequency portion of the spectrum. This enhancement is directly related to the fact that the peak heights in Fig. 2(a) fluctuate over a long time scale. It is important to point out that these feedback-induced fluctuations are present even when spontaneous-emission noise is neglected; i.e., the Langevin-noise sources in Eqs. (1) and (2) are turned off. The fluctuations caused by OFB are, thus, deterministic in nature. The resulting enhancement in the low-frequency part of the RIN spectrum is one of the signatures of a chaotic system, and this is shown with particular clarity in the bifurcation diagram shown in Fig. 3, which we now discuss.

The bifurcation diagram is a convenient method for showing the type of route to chaos followed by the system.<sup>13</sup> The diagram in Fig. 3 is calculated numerically for a single-mode laser using the parameters of Table 1 at a constant current of 65.7 mA. The bifurcation diagram is constructed in the following way: the solution to Eqs. (1) and (2) describes a trajectory in the 3-D  $(P, N, \phi)$  space; after the transients have died away, the intersections with a transverse reference plane are recorded; we have chosen  $P = P_s$ , where  $P_s$  is the average photon number for the solitary laser, as the reference plane. It is important to note that the Langevin noise sources are neglected in simulations used for making bifurcation diagrams. For small values of feedback,  $N$  and  $P$  approach a constant (fixed-point solution), so no intersection occurs with the reference plane. At a certain value of OFB, about a tenth of a percent of OFB in this case, the output power becomes periodic as the relaxation oscillations become undamped, and the result is a single point in the bifurcation diagram, because the  $P = P_s$  plane is crossed once during each cycle. At another critical value of OFB (near 0.2%), the laser begins a period-doubling route to chaos. Interestingly, the chaos disappears abruptly near 1% OFB, giving way to a region of frequency locking in which the output is once again stable and periodic. However, near 2% OFB, the process begins again, with another period-doubling route to chaos ending in a second frequency-locked state. During the third cycle of chaos, the laser follows a quasi-periodic route to chaos; the quasi-periodic route seems more prevalent for longer external cavities.<sup>13</sup> This pattern of chaotic regions interrupted by stable windows repeats itself many times as the feedback is increased. The particular positions where the stable windows appear depend on many parameters, notably on the linewidth enhancement factor  $\alpha$  and on the external-cavity length. The windows of stability, though interesting from a fundamental view, are not helpful in a practical system because the OFB varies considerably because of system imperfections. In the next section we discuss the elimination of the chaotic regimes by modulating the laser injection current, a technique known as high-frequency injection (HFI).

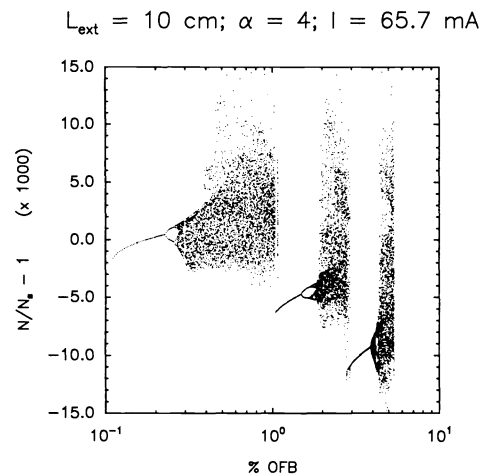


**Fig. 3** Bifurcation diagram for a single-mode laser showing the carrier number (normalized to the solitary laser value  $N_s$ ) as a function of increasing OFB.

#### 4 Control of Laser RIN by HFI

As discussed in the preceding section, the primary problem caused by OFB in optical recording systems is the increase in the low-frequency laser intensity noise, accompanied by a decrease in achievable SNR of the system. The dependence of laser intensity noise on OFB is shown in Fig. 4 for several decades of OFB. In this case, the low-frequency part of the RIN is averaged between 0 to 100 MHz. This curve was produced using the full multimode equations ( $M=5$ ) including noise. Because lasers in applications are often operated in constant power mode, the rest of the simulations are performed using a constant power of 1.6 mW. Similar to the bifurcation diagram, the total RIN shows regions of high noise interrupted by regions of frequency locking. The dashed line implies that the frequency-locked regions may not be observable in practice because of focusing errors, disk substrate nonuniformities, and other system imperfections. Simulations using the single-mode equations with these parameters reveal that the windows of frequency locking become narrower as the feedback is increased. Therefore, any amount of variation in the reflections at high feedback levels would manifest as large error bars in experimental RIN measurements.

The ultimate goal of the HFI technique is to make the laser intensity noise resilient to changes in OFB. There have been different interpretations of the method by which HFI achieves this goal. Some argue that HFI works because by the time the feedback returns to the laser the modulation has turned the laser off.<sup>6-8</sup> Such an interpretation implies that some modulation frequencies should work better than others. Others argue that HFI changes a laser operating in a single predominant mode (but suffering from mode hopping made worse by OFB) into a stable multimode laser,<sup>4,5</sup> which is known to have lower noise than a laser exhibiting mode hopping. Yamada and Higashi,<sup>9</sup> on the other hand, argue that HFI acts similar to spontaneous emission to weaken the competition between the modes; HFI is, thus, effective because it suppresses mode hopping, not because a multimode laser is produced.<sup>9</sup>

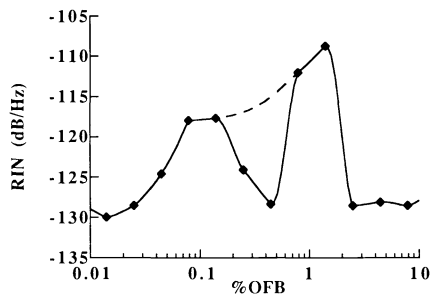


**Fig. 4** Low-frequency RIN versus OFB for a five-mode laser. The RIN, averaged between 0 to 100 MHz, shows regions of enhancement and windows of stability similar to bifurcation diagram. Dashed line shows the expected behavior when the stable windows are not resolved.

The point of view adopted in this paper, based on the bifurcation diagram in Fig. 3, is that the laser intensity noise increases because of deterministic chaos caused by coupling the laser to an external cavity—formed by the optical disk, in this case. For HFI to be effective, it must suppress or at least delay the onset of chaos so that the RIN remains near the solitary-laser value. The two HFI parameters that are user controllable to achieve this goal are the modulation frequency and the depth of modulation. Experimentally, the proper choice of frequency seems to be the more elusive parameter of the two. Whichever frequency is chosen, HFI must be able to suppress the increase in RIN for the large range of OFB strengths encountered in practice. To this end, we have calculated (Fig. 5) the average RIN as a function of HFI modulation frequency for three different levels of OFB: 0.15% and 1.4% correspond to the peaks in Fig. 4 and 0.5% represents a frequency-locked region. The simulations predict that modulating with a frequency near 500 MHz would serve to pin the laser noise to a low value for each of these levels of OFB. In fact, RIN is suppressed for all but the largest levels of OFB when modulated at 500 MHz. This is demonstrated in Fig. 6, which shows the importance of the depth of modulation for the HFI technique. The unmodulated case is shown for comparison. Generally speaking, HFI at the proper frequency serves to delay the onset of the feedback-induced chaos for each of the modulation depths shown toward very high feedback levels ( $\sim 10\%$ ), and the delay increases with the depth of modulation.

To compare the theoretical predictions to experiment, we have carried out measurements of the low-frequency RIN of an optical recording diode laser as a function of OFB using a range of HFI modulation frequencies and depths. As in the simulations, the external cavity length is 10 cm. The OFB is varied in the range of 0.1 to 10%, while the laser power is kept constant at 1.6 mW. In the experimental plots, each data point represents an average of the measurements of ten identical lasers; the error bars correspond to the standard deviation of this sample of ten lasers. By measuring the small-signal modulation response,<sup>2</sup> we have determined that only approximately 60% of the modulation current at 500 MHz is effective in driving the laser. This should be kept in mind when comparing the modulation depths employed experimentally with those of the simulations. Figure 7 shows RIN versus OFB for several different modulation frequencies, using a modulation depth of 40 mA

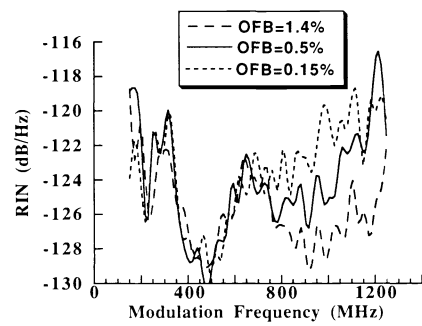


**Fig. 5** Dependence of low-frequency RIN on HFI modulation frequency for three levels of OFB. Modulation depth is 20 mA (peak to peak).

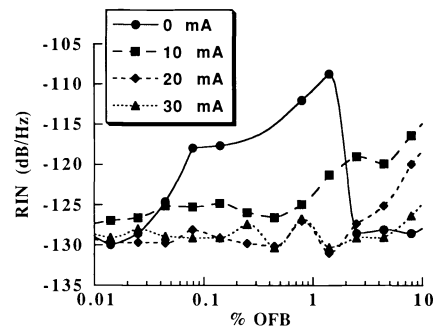


**Fig. 6** RIN versus OFB for three values of the modulation depth. Frequency of modulation chosen is 500 MHz based on Fig. 5.

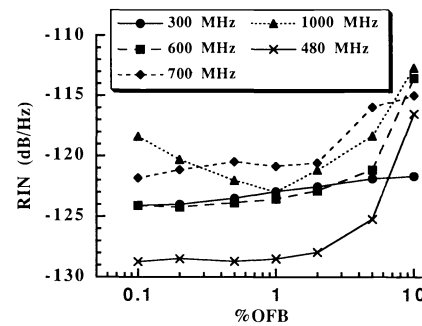


**Fig. 7** Experimental measurement of RIN versus OFB for five different modulation frequencies. Depth of modulation is 40 mA peak to peak.

(peak to peak). Of the five modulation frequencies shown, 480 MHz results in by far the greatest suppression of the RIN enhancement—the RIN remains below  $-125$  dB/Hz up to 5% OFB. Recall that the computer simulations predict (see Fig. 5) that a modulation frequency in the range 450 to 500 MHz gives the lowest values of RIN. Typical two-sided error bars for this plot are 3 to 4 dB.

The next experimental result, shown in Fig. 8, explores RIN versus OFB for different modulation depths using the modulation frequency of 480 MHz. The modulation depths shown are peak-to-peak values and are similar to the values used in the simulations. The unmodulated case is shown for comparison. The similarity of the experimental measurements to the simulated results in Fig. 6 are quite apparent.

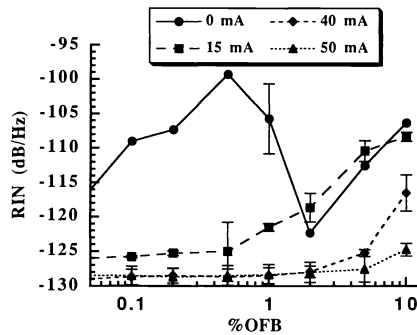


**Fig. 8** Experimental measurement of RIN versus OFB for different modulation depths, in comparison to Fig. 6.

With no modulation, the experimental RIN has already increased to high values for a feedback of 0.1%, similar to the simulations. At high feedback levels, the experimental RIN can actually decrease to low values, which corresponds to a frequency-locked state seen in the simulations. The experimental high feedback regime is very unstable, however, and the RIN fluctuates between high and low values. A typical error bar shown on the unmodulated RIN curve is 10 dB. This is consistent with the theoretical predictions that the frequency-locked states get narrower and closer together as OFB increases, so that variations in OFB switch the laser between states of chaos and frequency locking. When HFI is turned on, the transition of the RIN to high values is delayed as in the numerical simulations. For the levels shown here, larger modulation depths are more effective in delaying the onset of chaos, again in agreement with computer simulations.

## 5 Conclusions

Semiconductor lasers operating in optical recording systems or other applications suffer from unwanted reflections that are fed back into the laser. Such optical feedback can destabilize the laser intensity, leading to an increase in low-frequency RIN and subsequent reduction in the SNR of the optical recording system. Based particularly on single-mode laser results using the same parameters as the multimode case, we conclude that the increase in RIN with OFB arises from deterministic chaos caused by the coupling of the laser to an external cavity. The bifurcation diagram shows with increasing OFB a series of chaotic regions separated by windows of frequency locking. The frequency-locked states become narrower and closer together at high feedback and are not of practical use because feedback from the disk is not constant.

The common solution to this problem involves the modulation of the laser current at relatively high frequencies compared to the recording data rate. The effectiveness of the HFI technique rests in its ability to suppress or delay the onset of the chaotic regions, so that the RIN remains low. For proper choice of frequency and depth of modulation, the increase in RIN can be avoided. We have presented an optimization of this technique based on computer simulations of the multimode rate equations, modified to include OFB and HFI. Measured laser and system parameters are input to the program that calculates the total power RIN as a function of OFB. The suitable modulation fre-

quency for these parameters is then found. Experimental results are also given, and we find good agreement between them and the simulation results.

## Acknowledgments

We thank Scott Beckens for assistance with the experimental measurements and Dave Kay for technical advice. This work was supported by the New York State Center for Advanced Optical Technology. Computational support of the Cornell Supercomputing Center is also acknowledged.

## References

1. G. P. Agrawal and N. K. Dutta, *Semiconductor Lasers*, 2nd ed., Van Nostrand Reinhold, New York (1993).
2. K. Petermann, *Laser Diode Modulation and Noise*, Kluwer Academic, Boston (1991).
3. G. P. Agrawal, *Fiber-Optic Communication Systems*, Wiley, New York (1992).
4. T. Kanada, "Theoretical study of noise reduction effects by superimposed pulse modulation," *Trans. IECE Jpn.* **68**, 180-187 (1985).
5. K. Stubkjaer and M. B. Small, "Feedback-induced noise in index-guided semiconductor lasers and its reduction by modulation," *Electron. Lett.* **19**, 388-389 (1983).
6. A. Arimoto, M. Ojima, N. Chinone, A. Oishi, T. Gotoh, and N. Ohnuki, "Optimum conditions for the high frequency noise reduction method in optical videodisc players," *Appl. Opt.* **25**, 1398-1403 (1986).
7. M. Ojima, A. Arimoto, N. Chinone, T. Gotoh, and K. Aiki, "Diode laser noise at video frequencies in optical videodisc players," *Appl. Opt.* **25**, 1404-1410 (1986).
8. E. C. Gage and S. Beckens, "Effects of high frequency injection and optical feedback on semiconductor laser performance," *Proc. SPIE* **1316**, 199-204 (1990).
9. M. Yamada and T. Higashi, "Mechanism of the noise reduction method by superposition of high-frequency current for semiconductor injection lasers," *IEEE J. Quantum Electron.* **27**, 380-388 (1991).
10. G. P. Agrawal, "Gain nonlinearities in semiconductor lasers: theory and application to distributed feedback lasers," *IEEE J. Quantum Electron.* **QE-23**, 860-868 (1987).
11. R. Lang and K. Kobayashi, "External optical feedback effects on semiconductor injection laser properties," *IEEE J. Quantum Electron.* **QE-16**, 347-355 (1980).
12. R. W. Tkach and A. R. Chraplyvy, "Regimes of feedback effects in 1.5- $\mu$ m distributed feedback lasers," *J. Light. Technol.* **LT-4**, 1655-1661 (1986).
13. J. Mork, B. Tromborg, and J. Mark, "Chaos in semiconductor laser sixth optical feedback: theory and experiment," *IEEE J. Quantum Electron.* **28**, 93-108 (1992).

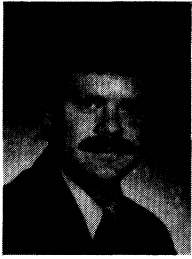


**George R. Gray** received the BA degree in physics and mathematics from Hanover College, Hanover, Indiana, in 1985. He received the MS and PhD degrees from the Georgia Institute of Technology in 1987 and 1990, respectively, where he held a presidential fellowship. His thesis dealt with longitudinal mode coupling and noise characteristics of solitary and external cavity semiconductor lasers. From 1990 to 1992 he was a research associate at The Institute of Optics, University of Rochester, New York. He is currently an assistant professor of electrical engineering at The University of Utah.

He has published papers on nonlinear gain and four-wave mixing in semiconductor lasers as well as the effects of normal and phase-conjugate optical feedback on the noise characteristics of semiconductor lasers. His research interests include semiconductor lasers, laser physics, nonlinear optics, quantum electronics, and optical recording. Dr. Gray is a member of APS, OSA, LEOS, and IEEE.

**Andrew T. Ryan** received his BS degree from the State University of New York College at Oswego, where he studied physics and mathematics. He has performed undergraduate research in optics at the Chemical Physics Institute at the University of Oregon in Eugene. He is currently working toward his PhD degree with Dr. Govind Agrawal at the Institute of Optics at the University of Rochester, New York.

**Govind P. Agrawal:** Biography and photograph of author appear with the special section guest editorial.



**Edward C. Gage** received the BA degree in physics from the State University of New York at Geneseo in 1983 and the MA and PhD degrees in physics from the University of Rochester, New York, in 1985 and 1989, respectively. The topic of his doctoral research was intensity fluctuations in one- and two-mode dye lasers. He has been with Eastman Kodak Company since 1989 as a research scientist in the Storage Technology Research and Development Division.

His research interests are in the areas of semiconductor laser physics and optical recording. Dr. Gage is a member of the OSA and the IEEE Lasers and Electro-Optics Society.